

Enhancing Computational Efficiency in State-Space Models Using Rao-Blackwellization and 2-Step Approximation

Genshiro Kitagawa

Tokyo University of Marine Science and Technology
and
The Institute of Statistical Mathematics

November 26, 2024

Abstract:

This paper explores a Bayesian self-organization method for state-space models, enabling simultaneous state and parameter estimation without repeated likelihood calculations. While efficient for low-dimensional models, high-dimensional cases like seasonal adjustment require many particles. Using Rao-Blackwellization and a 2-step approximation, the method reduces particle use and computation time while maintaining accuracy, as shown in Monte Carlo evaluations.

Key words: Nonlinear non-Gaussian state-space model; particle filter; smoother; multi-particle prediction; stratified sampling.

1 Introduction

The state-space model is a highly effective time-series model representation framework that can accommodate numerous time-series models in a unified manner. Moreover, once a linear Gaussian state-space representation is obtained, the state vector can be efficiently estimated sequentially from the observed data using a Kalman filter. This property enables the unified estimation of parameters, prediction, smoothing, decomposition into several components, and interpolation of missing values for time series models. Indeed, state-space models are employed in a multitude of fields, including seasonal adjustment methods, long-term prediction, and system control (Harison and Steevens (1976), West and Harrison (1989), Kitagawa and Gersch (1996), Shumway and Stoffer (2000), Durbin and Koopman (2012)).

Despite the considerable merits of the linear Gaussian state-space model, there is a clear need for improvement. Firstly, although the state-space model is a highly powerful tool with a wide range of applications, it requires extension to accommodate nonlinearities, asymmetries, structural changes, outliers, and the discreteness of observed values in the target system. Secondly, when the maximum likelihood method is employed to estimate the parameters of a state-space model, it typically represents a nonlinear optimisation problem, necessitating the completion of a vast number of likelihood calculations.

A self-organising state-space model has been put forth as a potential solution to this issue. In this approach, an unknown parameter vector is incorporated into the state vector of the original state-space model. By sequentially estimating this expanded state vector, it is possible to simultaneously estimate both the state vector and the structural parameters of the state-space model (Kitagawa, 1998). However, since the relationship between the structural parameters of the state-space model and the state vector is generally nonlinear, this state estimation cannot be achieved with a Kalman filter. Therefore, the use of nonlinear filters such as particle filters and non-Gaussian filters is necessary.

Although non-Gaussian filters that can be computed with a high degree of precision can address cases that can be expressed by low-dimensional state-space models, such as trend models, numerous significant problems, including seasonal adjustment methods and the decomposition

of time series, necessitate the utilisation of computational techniques such as particle filters. Particle filters have the significant advantage of being applicable to relatively high-dimensional nonlinear, non-Gaussian state-space models. However, this requires the use of a very large number of particles, which in turn necessitates lengthy computation times and substantial memory.

In this paper, as examples, we consider the problems of trend estimation and seasonal adjustment: the original purpose of Rao-Blackwellization is for practical applications in the case of high-dimensional state-space models such as seasonal adjustment models, but the reason for also showing the problem of trend estimation is that it can be computed almost exactly with NGF, even for self-organized state-space models. Therefore, it is possible to evaluate the estimated trend component.

This paper is organized as follows. Section 2 briefly introduces the state-space model and the problem of state estimation, the Kalman filter, the non-Gaussian filter and the particle filter. Section 3 introduces maximum likelihood estimation of state-space model parameters and self-organizing modeling methods, examines trend estimation and seasonal adjustment using examples, and evaluates their estimation accuracy and computation time through Monte Carlo experiments. Section 4 presents the Rao-Blackwellization approach for the piecewise linear state space model and shows examples of computations using particle and non-Gaussian filters for the trend estimation and seasonal adjustment problems, as well as Monte Carlo experiments demonstrating estimation accuracy and computation time. It is found that the number of particles can be reduced to 1/100 by RB, but it is also found that this does not always lead to a reduction in computation time when the dimension of the state space is high. To solve this problem, a two-step approximation method was developed. Monte Carlo experiments confirmed that this approximation can significantly reduce the computation time with little loss of estimation accuracy. Conclusions based on these results are presented in section 5.

2 A Brief Review of the Filtering and Smoothing Algorithms

2.1 The state-space model and the state estimation problems

Assume that a time series y_n is expressed by a linear state-space model

$$\begin{aligned} x_n &= F_n x_{n-1} + G_n v_n \\ y_n &= H_n x_n + w_n, \end{aligned} \tag{1}$$

where x_n is an k -dimensional state vector, v_n and w_n are ℓ -dimensional and 1-dimensional white noise sequences having density functions $q_n(v)$ and $r_n(w)$, respectively. The initial state vector x_0 is assumed to be distributed according to the density $p(x_0)$.

The information from the observations up to time j is denoted by Y_j , namely, $Y_j \equiv \{y_1, \dots, y_j\}$. The problem of state estimation is to evaluate $p(x_n|Y_j)$, the conditional density of x_n given the observations Y_j and the initial density $p(x_0|Y_0) \equiv p(x_0)$. For $n > j$, $n = j$ and $n < j$, it is called the problem of prediction, filtering and smoothing, respectively.

This linear state-space model can be generalized to a nonlinear non-Gaussian state-space model,

$$\begin{aligned} x_n &= F_n(x_{n-1}, v_n) \\ y_n &= H_n(x_n) + w_n, \end{aligned} \tag{2}$$

where $F_n(x, v)$ and $H_n(x)$ are possibly nonlinear functions of the state and the noise inputs, respectively. Diverse problems in time series analysis can be treated by using this nonlinear state-space model (Kitagawa and Gersch, 1996; Doucet et al., 2001).

2.2 The Kalman filter and the smoother

It is well-known that if all of the noise densities $q_n(v)$ and $r_n(w)$ and the initial state density $p(x_0)$ are Gaussian, then the conditional density of linear state-space model (1), the conditional density of x_n given Y_n , $p(x_n|Y_n)$, is also Gaussian and that the mean and the variance covariance matrix can be obtained by the Kalman filter and the fixed interval smoothing algorithms (Anderson and Moore, 1979).

To be specific, if we assume $q_n(v) \sim N(0, Q_n)$, $r_n(w) \sim N(0, R_n)$, $p(x_0|Y_0) \sim N(x_{0|0}, V_{0|0})$ and $p(x_n|Y_n) \sim N(x_{n|m}, V_{n|m})$, then the Kalman filter is given as follows:

One-step ahead prediction:

$$\begin{aligned} x_{n|n-1} &= F_n x_{n-1|n-1} \\ V_{n|n-1} &= F_n V_{n-1|n-1} F_n^T + G_n Q_n G_n^T. \end{aligned} \quad (3)$$

Filter

$$\begin{aligned} K_n &= V_{n|n-1} H_n^T (H_n V_{n|n-1} H_n^T + R_n)^{-1} \\ x_{n|n} &= x_{n|n-1} + K_n (y_n - H_n x_{n|n-1}) \\ V_{n|n} &= (I - K_n H_n) V_{n|n-1}. \end{aligned} \quad (4)$$

Using these estimates, the smoothed density is obtained by the following,

Fixed interval smoothing algorithm:

$$\begin{aligned} A_n &= V_{n|n} F_n^T V_{n+1|n}^{-1} \\ x_{n|N} &= x_{n|n} + A_n (x_{n+1|N} - x_{n+1|n}) \\ V_{n|N} &= V_{n|n} + A_n (V_{n+1|N} - V_{n+1|n}) A_n^T. \end{aligned} \quad (5)$$

2.3 The non-Gaussian filter and the smoother

It is well-known that for the nonlinear non-Gaussian state-space model (2), the recursive formulas for obtaining the densities of the one step ahead predictor, the filter and the smoother are as follows:

One step ahead prediction:

$$p(x_n|Y_{n-1}) = \int_{-\infty}^{\infty} p(x_n|x_{n-1}) p(x_{n-1}|Y_{n-1}) dx_{n-1}. \quad (6)$$

Filtering:

$$p(x_n|Y_n) = \frac{p(y_n|x_n) p(x_n|Y_{n-1})}{\int p(y_n|x_n) p(x_n|Y_{n-1}) dx_n}. \quad (7)$$

Smoothing:

$$p(x_n|Y_N) = p(x_n|Y_n) \int_{-\infty}^{\infty} \frac{p(x_{n+1}|Y_N) p(x_{n+1}|x_n)}{p(x_{n+1}|Y_n)} dx_{n+1}. \quad (8)$$

In Kitagawa (1987, 1988), an algorithm for implementing the non-Gaussian filter and smoother was developed by approximating each density function using a step-function or a continuous piecewise linear function and by performing numerical computations. This method was successfully applied to various problems such as estimation of trend or volatility, spectrum smoothing, smoothing discrete process and tracking problem (Kitagawa, 1987, 2020; Kitagawa and Gersch, 1996).

2.4 Sequential Monte Carlo filter and smoother for non-Gaussian nonlinear state-space models

The non-Gaussian filter and smoother based on numerical integration mentioned in the previous subsection has a limitation that it can be applied to only lower dimensional, such as the third or the fourth order, state-space model. Sequential Monte Carlo filter and smoother, hereinafter referred to as particle filter, were developed to mitigate this problem. In this method, each distribution appeared in recursive filter and smoother is approximated by many “particles” that can be considered as realizations from that distribution (Gordon et al., 1993; Kitagawa, 1993, 1996; Doucet et al., 2001).

In this paper, we use the following notations, $\{p_n^{(1)}, \dots, p_n^{(m)}\} \sim p(x_n|Y_{n-1})$, $\{f_n^{(1)}, \dots, f_n^{(m)}\} \sim p(x_n|Y_n)$, $\{s_{n|N}^{(1)}, \dots, s_{n|N}^{(m)}\} \sim p(x_n|Y_N)$. In practice, we approximate the cumulative distributions by the empirical distributions determined by the set of “particles”.

Then a recursive filtering algorithm is realized as follows:

1. Generate a k -dimensional random number $f_0^{(j)} \sim p_0(x)$, for $j = 1, \dots, m$.
2. Repeat the following steps for $n = 1, \dots, N$:
 - (a) Generate an ℓ -dimensional random number $v_n^{(j)} \sim q(v)$, for $j = 1, \dots, m$.
 - (b) Generate a new particle by $p_n^{(j)} = F(f_{n-1}^{(j)}, v_n^{(j)})$, for $j = 1, \dots, m$.
 - (c) Compute the importance weight $\alpha_n^{(j)} = r(y_n - H(p_n^{(j)}))$, of the particle $p_n^{(j)}$ for $j = 1, \dots, m$.
 - (d) Generate $f_n^{(j)} \sim (\sum_{i=1}^m \alpha_n^{(i)})^{-1} \sum_{i=1}^m \alpha_n^{(i)} I(x, p_n^{(i)})$, for $j = 1, \dots, m$ by the resampling of $p_n^{(1)}, \dots, p_n^{(m)}$ with the sampling rate proportional to $\alpha_n^{(n)}$.

3 Estimation of the Parameters and the State of the State-Space Model

3.1 Maximum Likelihood Estimation

Assume that the linear-Gaussian state-space model contains unknown parameter θ . The log-likelihood of the state-space model is given by

$$\begin{aligned} \ell(\theta) &= \log L(\theta) \\ &= -\frac{1}{2} \sum_{n=1}^N \log(2\pi r_n) - \frac{1}{2} \sum_{n=1}^N \frac{(y_n - Hx_{n|n-1})^2}{2r_n}, \end{aligned} \quad (9)$$

where $r_n = R_n + H_n V_{n|n-1} H_n^T$. Therefore, the maximum likelihood estimate of the parameter θ is obtained by maximizing this log-likelihood through numerical optimization.

3.2 Self-Organing State-Space Model

Assume that the state vector is x_n and the parameter of the state-space model is θ , and define an augmented state vector by

$$z_n = \begin{bmatrix} x_n \\ \theta \end{bmatrix}. \quad (10)$$

Then, by estimating the augmented state vector z_n , the state vector x_n and the parameter θ can be esimated simultaneously (Kitagawa, 1998).

Note that, since the state-space model for the augmented state vector z_n became nonlinear even if the original state-space model is linear, it is inevitable to use some nonlinear filtering method. Therefore, for the implementation of the self-organizing state-space model, it is necessary to apply non-Gaussian filter or particle filter mentioned in the previous subsections.

It is also noted that, it is rather natural to consider the parameter is time-varying and denote by θ_n . In that case, it is necessary to assume a model for the time evolution of the parameter, e.g., $\theta_n = \theta_{n-1} + u_n$, $u_n \sim N(0, \tau^2)$.

3.3 Examples

3.3.1 Trend Estimation

The left panel of Figure 1 shows the Japanese IIP, added value of plastic products from January 1981 to December 2007, $n=252$. For ease of presentation, 100 times the logarithmic value of the original data is actually considered. The right panel shows the estimate of the trend based on the first-order trend model

$$\begin{aligned} t_n &= t_{n-1} + v_n, & v_n &\sim N(0, \tau^2) \\ y_n &= t_n + w_n, & w_n &\sim N(0, \sigma^2), \end{aligned} \quad (11)$$

obtained by the seasonal adjustment program Decom (Kitagawa and Gersch, 1984). The maximum likelihood estimates are $\tau^2=0.1582$ and $\sigma^2=4.2624$ and the log-likelihood is -566.1999. Figure 1 shows the data and the estimated trend by theDecom. The thick line in the center indicates the mean value of the smoothed distribution, and the three lines outside it indicate $\pm 1, 2$, and 3 standard deviations, respectively.

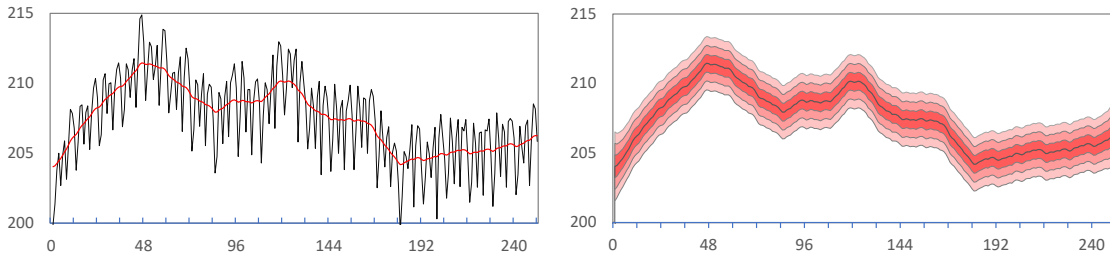


Figure 1: IIP-plastic products data and estimated trend by Decom. Left plot: data and estimated trend, right plot: Mean and $\pm 1, 2, 3$ standard error of the estimate.

The maximum likelihood method uses numerical optimization to obtain maximum likelihood estimates of parameters, which requires many iterations of likelihood calculations, whereas the self-organizing method provides the final posterior distribution by only one computation each of filtering and smoothing. However, since the self-organizing state-space models are generally nonlinear even when the original state-space model is linear, they cannot be computed with a Kalman filter, and require a non-Gaussian filter or a particle filter. For 2 or 3-dimensional state vectors such as those shown in Figure 2, a non-Gaussian filter can be used without problems, but if the original state vector is high-dimensional, it is difficult to apply a non-Gaussian filter.

Figure 2 shows the results of simultaneous estimation of trend and the variance of the system noise by the numerical integration based non-Gaussian filter and smoother. Define the augmented state vector z_n by

$$z_n = \begin{bmatrix} x_n \\ \theta_n \end{bmatrix}, \quad (12)$$

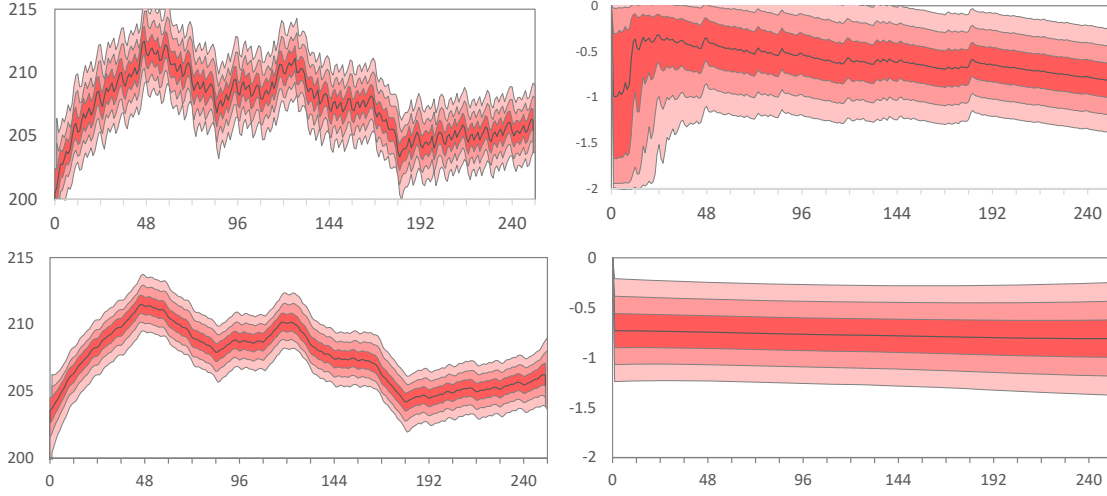


Figure 2: Trend estimation by self-organizing state-space model implemented by non-Gaussian filter and smoother.

where $\theta_n = \log \tau_n^2$. It is assumed that the time-varying parameter θ_n follows a random walk model $\theta_n = \theta_{n-1} + u_n$. Then the augmented state-space model is given by

$$\begin{bmatrix} x_n \\ \theta_n \end{bmatrix} = \begin{bmatrix} 1 & 0 \\ 0 & 1 \end{bmatrix} \begin{bmatrix} x_{n-1} \\ \theta_{n-1} \end{bmatrix} + \begin{bmatrix} \tau_n & 0 \\ 0 & 1 \end{bmatrix} \begin{bmatrix} v_n \\ u_n \end{bmatrix} \quad (13)$$

$$y_n = \begin{bmatrix} 1 & 0 \end{bmatrix} \begin{bmatrix} x_n \\ \theta_n \end{bmatrix} + w_n, \quad (14)$$

where $v_n \sim N(0, 1)$, $w_n \sim N(0, \sigma^2)$. At first, we consider the case where the observation noise variance is known to be $\sigma^2 = 4.2624$. Note that, by setting the system noise variance for u_n to 0, the case where τ^2 is a constant can also be treated by the self-organizing state-space model.

The upper two plots of Figure 2 show the marginal posterior distribution obtained by the non-Gaussian filter and the lower plots show the ones by the non-Gaussian smoother with $k_1 = 401$ and $k_2 = 101$. The upper left plot shows the estimated trend $t_{n|n}$, and the upper right shows the estimated $\log \tau_{n|n}^2$ (mean and $\pm 1, 2, 3$ standard deviation of the posterior distribution). The trend estimates are highly variable. Filtered distribution of the logarithm of the system noise variance, $\log \tau^2$, is initially very broad ranging from -2 to 0 and larger, but as the number of data n increases, the mean value converges to around -0.8 .

The smoothed distribution of the trend shown in the lower left plot is almost identical to that in Figure 1. In addition, the distribution of $\log \tau^2$ is almost constant over time. Note that The maximum likelihood estimate of the system noise variance was 0.1582 , i.e., $\log \hat{\tau}^2 = -0.8008$. Also, it is worth noting that the distribution of system noise is quite different for filtering and smoothing.

Figure 3 shows the posterior distributions obtained by the particle filter for the same two-dimensional self-organizing state-space model as in Figure 2. The number of particles is $m = 10^6$. The top two plots show the case of the filter estimate, and the bottom plots show the case of fixed-lag smoothing with $\text{lag}=252$. Using a very large number of particles, $mp = 1,000,000$, gives good results that are visually indistinguishable from the results for non-Gaussian filter and smoother, which gives almost exact results.

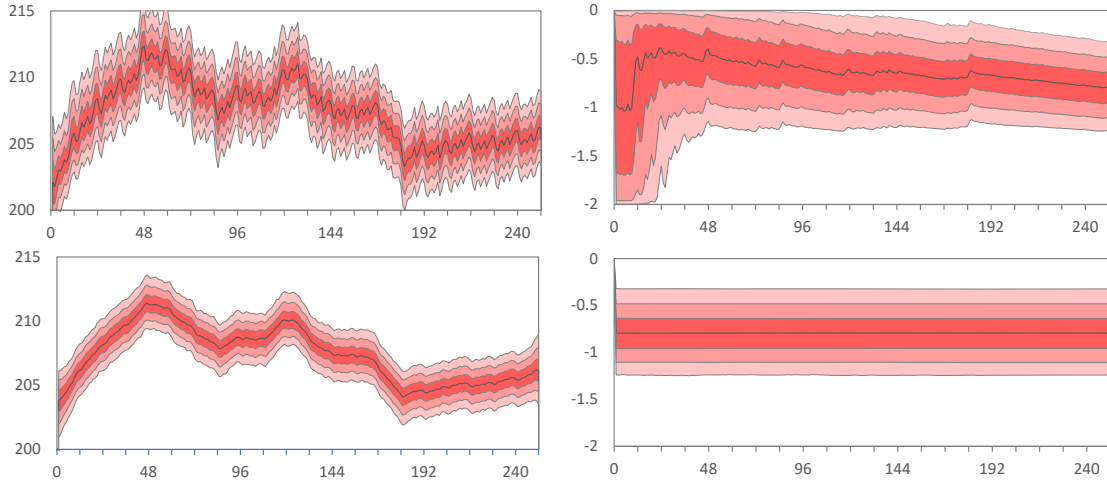


Figure 3: Trend estimation by self-organizing state-space model implemented by particle filter (upper plots) and smoother (lower plots) with number of particles $mp=1,000,000$.

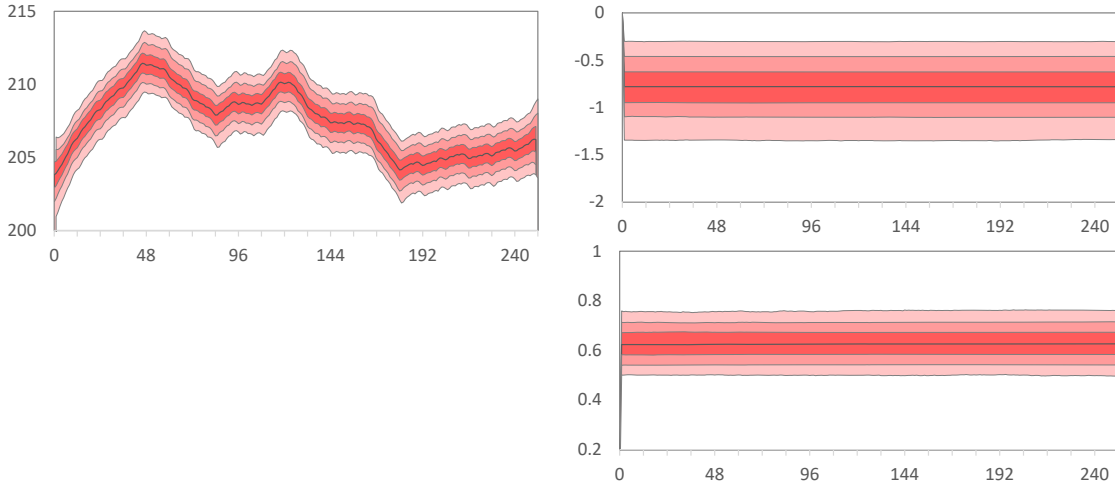


Figure 4: Trend estimation by 3-dimensional self-organizing state-space model implemented by particle smoother with number of particles $mp=1,000,000$. Left plot: trend, upper right plot: $\log \tau_n^2$, lower right: $\log \sigma_n^2$.

Note that by defining a two dimensional parameter vector by

$$\theta_n = \begin{bmatrix} \log \theta_n^2 \\ \log \sigma_n^2 \end{bmatrix}, \quad (15)$$

it is possible to estimate the state vector, the system and observation noise variances, simultaneously. Figure 4 shows particle smoother estimates of 3-dimensional self-organizing state-space model with $mp=1,000,000$ and $lag=252$. The posterior distribution of trend and system noise variance is almost the same as in Figure 3. The mean value, around 0.6, of the posterior distribution of the observed noise variance $\log \sigma_n^2$ corresponds to the logarithm of the maximum likelihood estimate, $\log_{10} 4.2642=0.63$.

In the following, we numerically evaluate the relationship between the number of particles in the particle filter or the number of nodes for non-Gaussian filter and the trend estimation error and computation time.

Table 1: Estimation errors of posterior mean. NGF: Non-Gaussian filter, PF: particle filter, 1D-SOF: Self-organizing state-space model with 1-dimensional parameter, 2D-SOF: with 2-dimensional parameter.

Method	Nodes/mp	Estimation error of trend			cpu-time	
		log-lk	Filter	Smoother	Filter	Smoother
NGF 1D-SOF	201×101	−566.693	0.1128	0.1794	1.8438	1.6563
	401×101	−566.646	0.0281	0.0460	6.1563	5.6875
	801×101	−566.626	0.0080	0.0142	22.4219	20.7813
	1601×101	−566.616	0.0037	0.0071	85.4531	79.0156
	3201×101	−566.612	0.0029	0.0058	333.5000	307.3125
PF 1D-SOF	1,000	−566.813	1.0199	7.5362	0.0313	0.1563
	10,000	−566.724	0.1035	0.8412	0.3750	2.1250
	100,000	−566.689	0.0090	0.0852	3.6719	19.8594
	1,000,000	−566.681	0.0010	0.0084	36.2656	215.7188
NGF 2D-SOF	201×25×25	−569.322	0.1039	0.1714	10.5781	9.7188
	401×25×25	−569.266	0.0246	0.0404	36.7344	33.8594
	801×25×25	−569.242	0.0054	0.0088	136.5469	124.1406
	1601×25×25	−569.232	0.0010	0.0016	530.5469	473.2813
	3201×25×25	−569.226	0.0001	0.0002	2073.6719	1831.9219
PF 2D-SOF	1,000	−569.653	2.2418	14.8492	0.0625	0.3438
	10,000	−569.054	0.1880	1.9205	0.6406	3.6719
	100,000	−569.000	0.0211	0.2098	6.3750	36.2500
	1,000,000	−568.997	0.0025	0.0223	64.6250	384.0469

Table 1 shows the change in estimation errors of the trend component with the number of nodes in the numerical integration method and with the number of particles, mp , in the particle filter. Trend estimation error was evaluated by

$$E_1 = \sum_{n=1}^N (\hat{t}_n - t_n^*)^2 \quad (16)$$

where N is the data length, \hat{t}_n is the posterior mean of the trend and t_n^* is the “true” trend value. Here, an approximate “true” trend is obtained by averaging 10 repetitions of a particle filter with 10,000,000 particles using different random numbers, since the results of the particle filter depend on the random numbers. Also in the evaluation of the particle filter, we repeat the estimation $nrep$ times with different random numbers and show their averages ($nrep=100$ for $mp=1,000$ and 10,000, $=25$ for $mp=100,000$ and $=10$ for $mp=1,000,000$). Since the computation of the non-Gaussian filter is deterministic, it is not necessary to repeat the computation. The log-likelihood value and cpu-time measured at ordinary PC (3.20GHz, 32GB RAM) are also shown.

2D-SOF is the case where the logarithm of the system noise variance and the logarithm of the observed noise variance are unknown, while 1D-SOF is the case where the observed noise variance is known (maximum likelihood estimate: $\sigma^2=4.2642$).

By NGF, the numerical integration method, in both cases of 1D-SOF and 2D-SOF, the error rapidly decreases as the number of nodes increases. In this table, the number of nodes in the NGF is increased only for the part corresponding to the trend component and kept constant for the part corresponding to the noise variance. This is because, although not shown in this table,

increasing the number of nodes corresponding to the variance parameters further has little effect, and in fact, decreasing the number to 51 or even lower yields almost the same accuracy. On the other hand, in the case of particle filters, increasing the number of particles to $mp = 10,000$ or more does not result in a noticeable decrease in error. In the case of non-Gaussian filter, if the number of Nodes is doubled, the error variance becomes about 1/3 to 1/5. On the other hand, in the case of particle filter, the error variance becomes about 1/10 when the number of particles is increased by a factor of 10.

With respect to cpu time, for non-Gaussian filter, the cpu-time increases with the square of the total number of nodes and for particle filter, cpu-time increases in proportion to the number of particles.

3.3.2 Seasonal Adjustment

Here we consider the seasonal adjustment model as an example of a case where the original state vector is high-dimensional. Left plots of Figure 5 shows the results of seasonal adjustment of Bslallhood data (Kitagawa, 2010) using the Decomp model with a trend order of 2 and a seasonal component order of 1:

$$\begin{aligned} T_n &= 2T_{n-1} - T_{n-2} + v_n \\ S_n &= -(S_{n-1} + \dots + S_{n-11}) + u_n \\ y_n &= T_n + S_n + w_n, \end{aligned} \tag{17}$$

where T_n and S_n are trend and seasonal component, respectively, and $v_n \sim N(0, \tau_1^2)$, $u_n \sim N(0, \tau_2^2)$ and $w_n \sim N(0, \sigma^2)$.

The left plot is obtained by a particle filter using the maximum likelihood estimates: $\tau_1^2 = 0.521 \times 10^{-2}$, $\tau_2^2 = 0.8069$, $\sigma^2 = 29.521$. On the other hand, the right plot is obtained by the self-organizing state-space model using the particle filter with $mp=100,000$, $lag=156$. 4th-6th plots from the top show the time variation of τ_1^2 , τ_2^2 , and σ^2 , respectively.

Table 2 shows the change in estimation error and cpu time with respect to changes in the number of particles in a 16-dimensional self-organizing state-space model consisting of a 13-dimensional state vector, two system variances, and an observed noise variance. The estimation error was evaluated by

$$E_2 = \frac{1}{1000} \left\{ \sum_{n=1}^N (\hat{t}_n - t_n^*)^2 + \sum_{n=1}^N (\hat{s}_n - s_n^*)^2 \right\}, \tag{18}$$

where the “true” values t_n^* and s_n^* were approximated by the average of 10 runs of the particle filter with $mp=4,000,000$. It can be seen that when the number of particles is increased by a factor of 10, the approximation error becomes about 1/3, but the computation time increases by a factor of 10.

Table 2: Estimation errors of seasonal adjustment model.

Method		Accuracy			cpu-time	
		log-lk	Filter	Smoother	Filter	Smoother
PF-3DSOF	1,000	-626.803	4.1993	4.8192	0.094	0.219
	10,000	-616.856	0.7288	1.3815	0.813	3.297
	100,000	-614.222	0.2524	0.6708	7.875	27.875
	1,000,000	-613.199	0.0702	0.2941	79.922	314.422

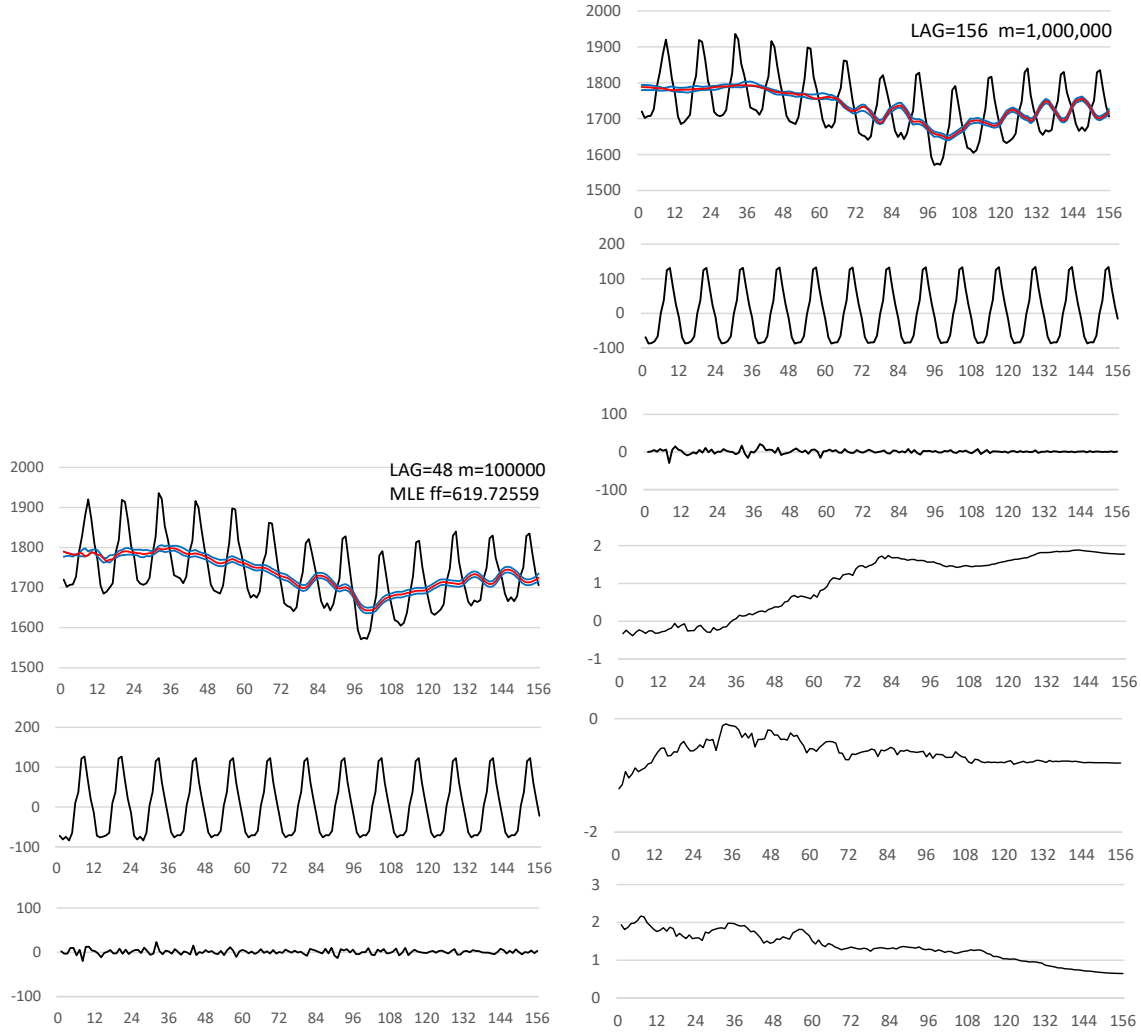


Figure 5: Seasonal adjustment of Blsallfood data by Decomp (left) and Self-organizing state-space model with particle filter.

4 Partially Linear State-Space Model

As shown in the previous section, if the state-space model has a parameter θ , by defining the augmented state vector as

$$z_n = \begin{bmatrix} x_n \\ \theta_n \end{bmatrix} \quad (19)$$

and by applying a filter such as particle filter and the non-Gaussian filter, the state and parameters can be estimated simultaneously. However, these methods are computationally expensive and memory intensive especially when the dimension of the state vector is high.

A clue to solving this problem is that the original state-space model is linear-Gaussian, and given the parameters θ_n , a computationally efficient Kalman filter can be applied. Namely, in our case, the self-organizing state-space model can be expressed as the following partially linear

state-space model

$$\begin{aligned}
x_n &= F_n(\theta_{n-1})x_n + G_n(\theta_{n-1})v_n \\
\theta_n &= J_n(\theta_{n-1}) + u_n \\
y_n &= H_n(\theta_{n-1}) + w_n,
\end{aligned} \tag{20}$$

where $v_n \sim N(0, Q_n(\theta_{n-1}))$, $u_n \sim N(0, S_n(\theta_{n-1}))$, $w_n \sim N(0, R_n(\theta_{n-1}))$. $F_n(\theta_{n-1})$, $G_n(\theta_{n-1})$ and $H_n(\theta_{n-1})$ are $(m+l) \times (m+l)$, $(m+l) \times (k+l)$ and $1 \times (m+l)$ dimensional matrices, respectively. $J_n(\theta_{n-1})$ is an appropriate function of the previous state θ_{n-1} . In the current examples, we use a random walk model for the parameter, i.e., $J_n(\theta_{n-1}) = \theta_{n-1}$.

4.1 Rao-Blackwellization

Here is the revised version of your text for improved clarity and readability:

Filtering in the self-organizing state-space model involves nonlinear computations, requiring the use of nonlinear filtering and smoothing methods such as particle filters or non-Gaussian filters. However, as demonstrated earlier, the original state-space model is linear Gaussian, allowing portions of the computation to be efficiently handled using the Kalman filter (Doucet et. al., 2000; Hendeby et. al., 2010; Särkkä et al., 2007).

Notably, when the dimension of the state vector exceeds that of the parameter vector, computational efficiency can be significantly enhanced by leveraging partial linearity in the computations.

In fact, the predictive and filter distributions can be expressed as follows:

$$\begin{aligned}
p(z_n|Y_{1:n-1}) &= p(x_n, \theta_n|Y_{1:n-1}) \\
&= \int \int p(x_n, x_{n-1}, \theta_n, \theta_{n-1}|Y_{1:n-1}) dx_{n-1} d\theta_{n-1} \\
&= \int \int p(\theta_n|x_n, x_{n-1}, \theta_{n-1}) p(x_n|x_{n-1}, \theta_{n-1}) p(x_{n-1}, \theta_{n-1}|Y_{1:n-1}) dx_{n-1} d\theta_{n-1} \\
&= \int p(\theta_n|\theta_{n-1}) \int p(x_n|x_{n-1}, \theta_{n-1}) p(x_{n-1}|\theta_{n-1}, Y_{1:n-1}) dx_{n-1} p(\theta_{n-1}|Y_{1:n-1}) d\theta_{n-1} \\
&= \int p(\theta_n|\theta_{n-1}) p(x_n|\theta_{n-1}, Y_{1:n-1}) p(\theta_{n-1}|Y_{1:n-1}) d\theta_{n-1}.
\end{aligned} \tag{21}$$

$$\begin{aligned}
p(z_n|Y_{1:n}) &= p(x_n, \theta_n|y_n, Y_{1:n-1}) \\
&\propto p(y_n, x_n, \theta_n|Y_{1:n-1}) \\
&= p(y_n|x_n, \theta_n, Y_{1:n-1}) p(x_n, \theta_n|Y_{1:n-1}) \\
&= p(y_n|x_n, \theta_{n-1}) p(x_n, \theta_n|Y_{1:n-1}),
\end{aligned} \tag{22}$$

where $p(x_n|\theta_{n-1}, Y_{1:n-1})$, $p(x_n|x_{n-1}, \theta_{n-1})$ and $p(y_n|x_n, \theta_{n-1})$ can be obtained by the Kalman

filter given θ_{n-1} . The smoothing can be realized as follows:

$$\begin{aligned}
p(z_n|Y_{1:N}) &= \int_{-\infty}^{\infty} p(z_n, z_{n+1}|Y_{1:N}) dz_{n+1} \\
&= \int \int p(x_n, x_{n+1}, \theta_n, \theta_{n+1}|Y_{1:N}) dx_{n+1} d\theta_{n+1} \\
&= \int \int p(x_n, x_{n+1}|\theta_n, \theta_{n+1}, Y_{1:N}) p(\theta_n, \theta_{n+1}|Y_{1:N}) dx_{n+1} d\theta_{n+1} \\
&= \int \int p(x_n, x_{n+1}|\theta_n, Y_{n+1:N}) p(\theta_n, \theta_{n+1}|Y_{1:N}) dx_{n+1} d\theta_{n+1} \\
&= \int p(x_n, x_{n+1}|\theta_n, Y_{n+1:N}) dx_{n+1} \int p(\theta_n, \theta_{n+1}|Y_{1:N}) d\theta_{n+1} \\
&= \int p(x_n|x_{n+1}, \theta_n, Y_{n+1:N}) p(x_{n+1}|\theta_n, Y_{n+1:N}) dx_{n+1} \times p(\theta_n|Y_{1:N}) \\
&= \int p(x_n|x_{n+1}, \theta_n) p(x_{n+1}|\theta_n, Y_{n+1:N}) dx_{n+1} \times p(\theta_n|Y_{1:N}) \\
&= p(x_n|\theta_n, Y_{1:N}) p(\theta_n|Y_{1:N}). \tag{23}
\end{aligned}$$

Here, $p(x_n|\theta_n, Y_{1:N}) = \int p(x_n|x_{n+1}, \theta_n) p(x_{n+1}|\theta_n, Y_{n+1:N}) dx_{n+1}$ can be obtained by the Kalman smoothing.

On the other hand, the update of the parameter θ_n is computed with a particle filter or a non-Gaussian filter. In the seasonal adjustment example in the previous section, the dimension of the state vector z_n is 16, of which the dimension of the state vector x_n is 13 and the dimension of the parameter vector θ_n is 3. In this case, using the Rao-Blackwellization, the calculation of the 13-th dimension can be performed using the computationally efficient Kalman filter, and only a numerical calculation of the third dimension is required, thus achieving a very efficient calculation.

4.2 Trend estimation

In this subsection, we present the results of the calculations using Rao-Blackwellization for the trend estimation presented in Subsection 3.3.

4.2.1 Implementation by Particle Filter and Smoother

Figure 6 shows the filter and smoothing estimates of the Rao-Blackwellized state-space model implemented by a particle filter with $mp=10,000$. The left side plots show the posterior distributions of the trend and the right plots show the posterior distributions of the logarithm of the system noise variance. The upper panels show the filter estimates, and the lower panels show the smoothing estimates. As shown in the previous section, the direct particle filter calculation requires a large number of particles, such as $mp = 100,000$ or $1,000,000$, while Rao-Blackwellized state-space model provides an equivalent estimates even with $mp = 10,000$.

In practice, as shown in Figure 7, even a much smaller number of particles, such as $mp = 100$ or 1000 , would yield almost similar results with respect to trend estimation. However, for the logarithm of the system noise calculated by the particle filter, there is a degeneracy of the posterior distribution, especially for $mp = 100$. It is interesting to note that even in such cases, when the mean of the logarithm of the system noise variance is nearly accurate, the trend estimation is, at least visually, quite accurate.

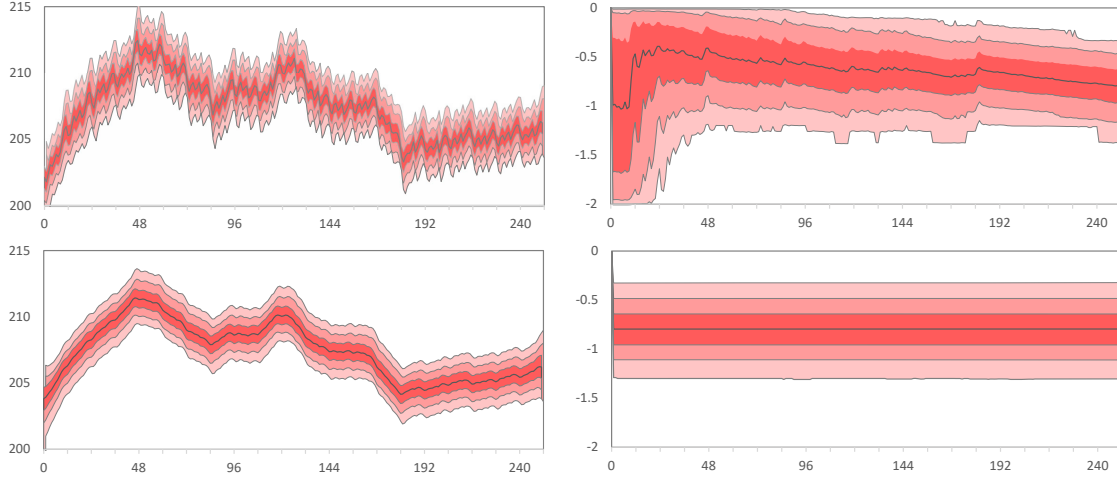


Figure 6: Trend and parameter estimation by 1 parameter RB-SOF particle filter with $mp=100,000$. Upper plots: filter, lower plots: smoother. Left plots: trend, right plots: logarithm of system noise variance.

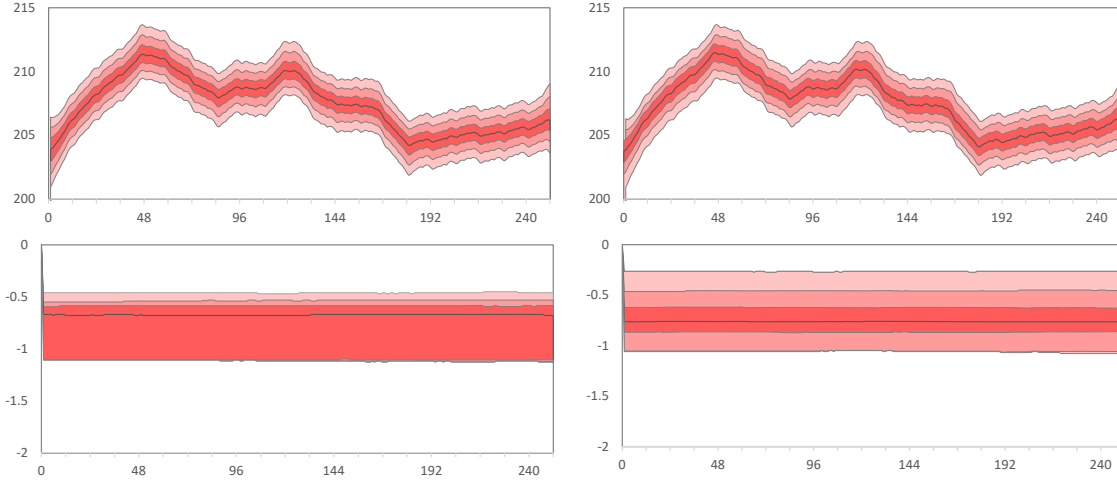


Figure 7: Trend estimation by RB-SOF modeling with 1 parameters, $mp=100$ (left) and 1,000 (right).

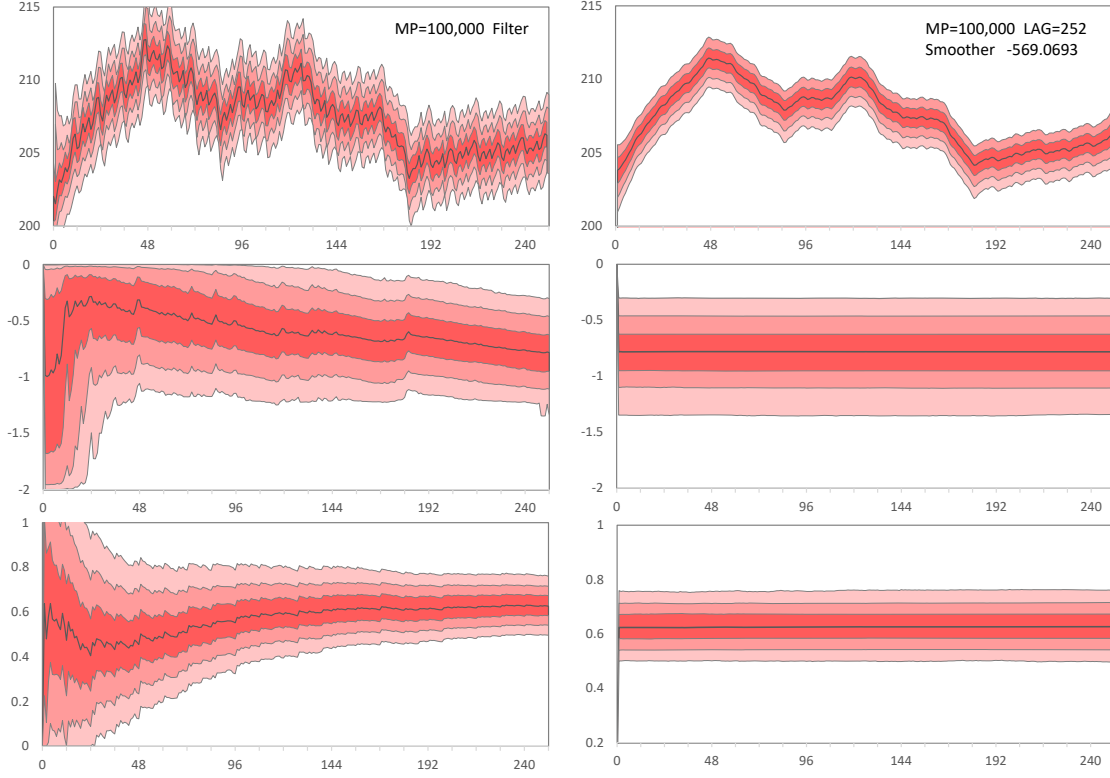


Figure 8: Trend estimation by RB-SOF modeling with 2 parameters, NP=10000.

Figure 8 shows the case of a self-organizing state-space model with two-dimensional parameter consisting of the logarithm of the system noise variance and the observation noise variance. Comparison with Figure 4 shows that Rao-Blackwellization yields good estimates even for two-dimensional parameters where the variances of the system noise and the observed noise are also unknown.

Table 3 shows the sum of squared errors and cpu-time of the trend by Rao-Blackellized state-space model. Particle filter (PF) and numerical integration based non-Gaussian filter (NGF) are used for both one-parameter case and two-parameter case.

Compared to Table 1, the squared error of trend is small even when the number of nodes and particles is small, indicating that only about 1/100 of the number of particles is needed to achieve the same accuracy. This is due to the fact that the state estimation of the trend is computed rigorously by the Kalman filter, while it is the variance parameter that is computed numerically by PF or NGF.

As for cpu-time, a smaller estimation error can be obtained with a smaller number of nodes or particles, indicating that a significant reduction of computation time can be achieved. With Rao-Blackwellization, necessary number of nodes in NGF is 101 for 1D-parameter case, 25×25 for 2D-parameter case, and about 1000 particles in PF is sufficient. Therefore, it can be seen that the computation time can be significantly reduced by using Rao-Blackwellization in order to achieve the same level of estimation error.

Table 3: Squared errors of posterior means and cpu-time of Rao-Blackwellized filtering

Filter Method	mp	Accuracy			cpu-time	
		log-lik	Filter	Smoother	Filter	Smoother
NGF-RB-1DSOF	11	-566.786	0.0452	0.0103	0.0022	0.0000
	25	-566.732	0.0133	0.0103	0.0039	0.0000
	101	-566.654	0.0010	0.0056	0.0109	0.0000
	201	-566.669	0.0023	0.0072	0.0250	0.0063
	401	-566.660	0.0019	0.0075	0.0641	0.0359
PF-RB-1DSOF	100	-566.856	0.5681	0.4539	0.0156	0.0156
	1,000	-566.720	0.0557	0.0441	0.0781	0.0781
	10,000	-566.689	0.0054	0.0049	0.7188	0.7500
	100,000	-566.686	0.0006	0.0004	6.6563	6.9375
NGF-RB-2DSOF	11×11	-568.905	0.1318	0.0123	0.0094	0.0000
	25×25	-568.821	0.0302	0.0009	0.0375	0.0016
	51× 51	-568.788	0.0109	0.0009	0.1734	0.0016
	101×101	-568.736	0.0004	0.0005	0.9188	0.0172
	201×201	-568.768	0.0011	0.0001	5.6734	0.0688
PF-RB-2DSOF	100	-570.063	2.7197	3.0128	0.0156	0.0000
	1,000	-569.089	0.1998	0.2109	0.2188	0.0000
	10,000	-569.003	0.0187	0.0210	2.4688	0.0000
	100,000	-568.991	0.0021	0.0035	23.0781	0.0781

Table 4: Effect of Rao-Blackwellization: comparison of trend estimation errors and cpu-times of simple filtering and Rao-Blackwellized filtering.

Filter Method	Simple State-Space Model			Roa-Blackwellized SSM		
	Mesh	Accuracy	Cpu-time	Mesh	Accuracy	Cpu-time
NGF-RB-1DSOF	201× 101	0.1794	1.6563	11	0.0103	0.0022
	401× 101	0.0460	5.6875	25	0.0103	0.0039
	801× 101	0.0142	20.7813	101	0.0056	0.0109
	1601× 101	0.0071	79.0156	201	0.0072	0.0313
	3201× 101	0.0058	307.3125	401	0.0075	0.1000
PF-RB-1DSOF	1,000	7.5362	0.1563	100	0.4539	0.0156
	10,000	0.8412	2.1250	1,000	0.0441	0.0781
	100,000	0.0852	19.8594	10,000	0.0049	0.7500
	1,000,000	0.0084	215.7188	100,000	0.0004	6.9375
NGF-RB-2DSOF	201× 25×25	0.1714	9.7188	11×11	0.0123	0.0094
	401× 25×25	0.0404	33.8594	25×25	0.0009	0.0391
	801× 25×25	0.0088	124.1406	51×51	0.0009	0.1750
	1601× 25×25	0.0016	473.2813	101×101	0.0005	0.9360
	3201× 25×25	0.0002	1831.9219	201×201	0.0001	5.7422
PF-RB-2DSOF	1,000	14.8492	0.3438	100	3.0128	0.0156
	10,000	1.9205	3.6719	1,000	0.2109	0.2188
	100,000	0.2098	36.2500	10,000	0.0210	2.4688
	1,000,000	0.0223	384.0469	100,000	0.0035	23.1562

4.2.2 Implementantion by Non-Gaussian Filter and Smoother

We consider here the trend estimation using a self-organizing state-space model and a non-Gaussian filter based on numerical integration. Only results for the 2D-parameter model are shown. Since the trend model has two parameters τ^2 and σ^2 , we put $\theta = (\log_{10} \tau^2, \log_{10} \sigma^2)^T$. We assume $-2.5 \leq \log_{10} \tau_n^2 \leq 1.0$ and $0 \leq \log_{10} \sigma_n^2 \leq 1$. These region are divided into k sub-interval. So there are k^2 sub-divisions in 2-D space.

Figure 9 shows the results for $k = 101$. Left plots show the posterior distribution of the filter, and the right plots those of smoother. From top to bottom, each plot shows the posterior distribution of the trend, logarithm of the system noise variance, and logarithm of the observation noise variance. We can see that Rao-Blackwellization yields the same results as in Figure 4.

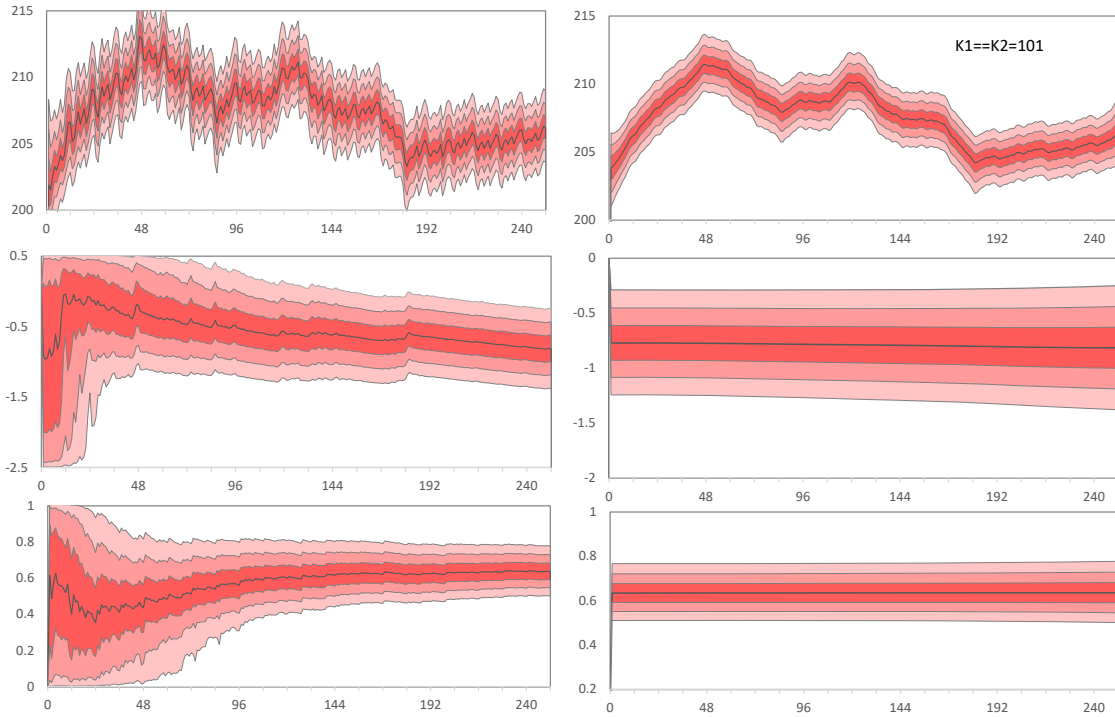


Figure 9: Trend estimation by RB-SOF modeling by non-Gaussian filter (left plots) and smoother (right plots), $k_1 = k_2=101$. From top to bottom, posterior distributions of trend, $\log \tau_n^2$ and $\log \sigma_n^2$.

From Table 3, it can be seen that the same accuracy as in the Table 1 can be obtained with as few as 25 node points. This corresponds to the fact that in Table 1, a large number of nodes was necessary for the trend component but not for the noise variances. In other words, since the Kalman filter can accurately estimate the trend component, it is not necessary to use a very large number of nodes for the noise variances.

Table 4 contrasts the estimation errors and cpu-time with simple state-space model and the Rao-Blackwellized state-space model. From this table we can see the following:

- In the case of a non-Gaussian filter based on numerical integration, high accuracy can be obtained even with a very small number of nodes (such as $k=25$) by Rao-Blackwellization, and a significant reduction in cpu-time can be achieved. On the other hand, increasing the number of nodes does not improve the estimation accuracy much.
- For particle filter, Rao-Blackwellized state-space model can achieve better estimation ac-

curacy than simple state-space model even with 100 or 1,000 particles, resulting in a remarkable reduction of computation time.

Figure 10 displays the same results in a scatter plots, with the logarithm of the estimation error on the vertical axis and the logarithm of the cpu-time on the horizontal axis. The left side is the one-parameter model and the right side is the two-parameter model. By Rao-Blackwellization (RB-PF), the same level of accuracy can be attained in about 1/100 of the computation time of the particle filter (PF). In the case of the non-Gaussian filter (NGF), it is also possible to achieve a speed-up of more than 100 times, but especially in the case of the one-parameter model, there is no improvement in accuracy even if more nodes are added and computation time is used.

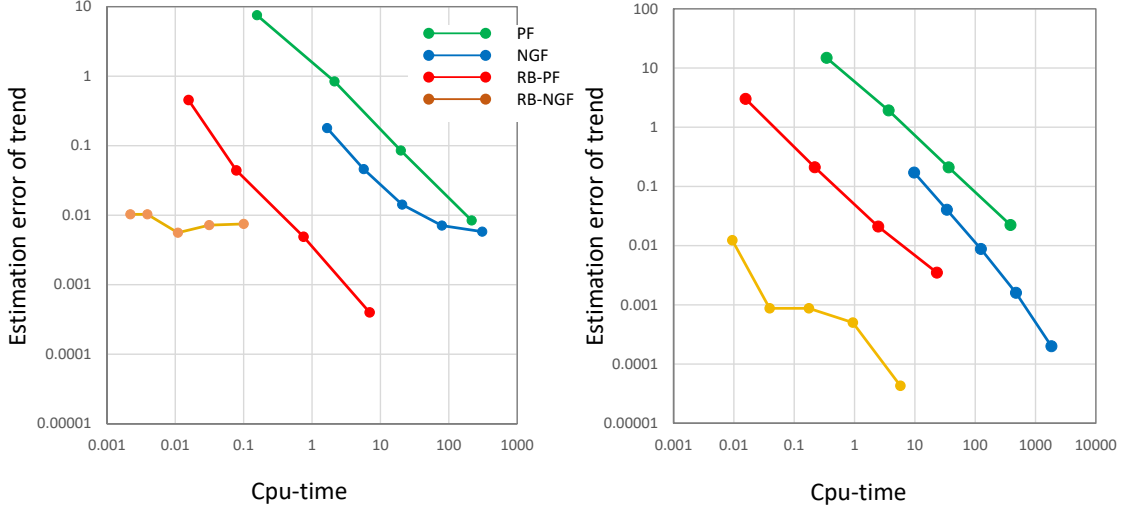


Figure 10: Cpu-time vs. estimation error of the trend. Left: 1D-parameter model, right: 2D-parameter model.

4.3 Seasonal adjustment

Figure 11 shows the Rao-Blackwellized self-organizing estimates of the seasonal adjustment model with a particle filter (left) and non-Gaussian filter (right). The state vector for the seasonal adjustment model is defined by $x_n = (T_n, T_{n-1}, S_n, \dots, S_{n-11})^T$. On the other hand, this model contains three parameters, the variance of the system noise for the trend model, τ_1^2 , the variance of the system noise for the seasonal component model, τ_2^2 and the variance of the observation noise, σ^2 . In actual computation, the logarithm of the variances are considered as the parameters. Therefore, the parameter vector is $\theta_n = (\log_{10} \tau_1^2, \log_{10} \tau_2^2, \log_{10} \sigma^2)$, and the augmented state $z_n = (x_n^T, \theta_n^T)^T$ becomes 16 dimensional.

Left plots of Figure 11 shows the results of Rao-Blackwellized seasonal adjustment using a self-organizing state-space modeling by a particle filter with 10,000 particles. From top to bottom, data and trend, seasonal component, noise, $\log \tau_1^2$, $\log \tau_2^2$, and $\log \sigma^2$ are shown. The red line shows the mean and the blue line shows the ± 2 standard error.

Looking at the trend estimation results, unlike the results in Figure 5, where the entire trend was estimated with a particle filter, there is no reduction in the error width of the trend even though only 1/100 of particles are used. From this, it can be inferred that Rao-Blackwellization improves the accuracy of smoothing. As for the structural parameters, as in Figure 5, we see

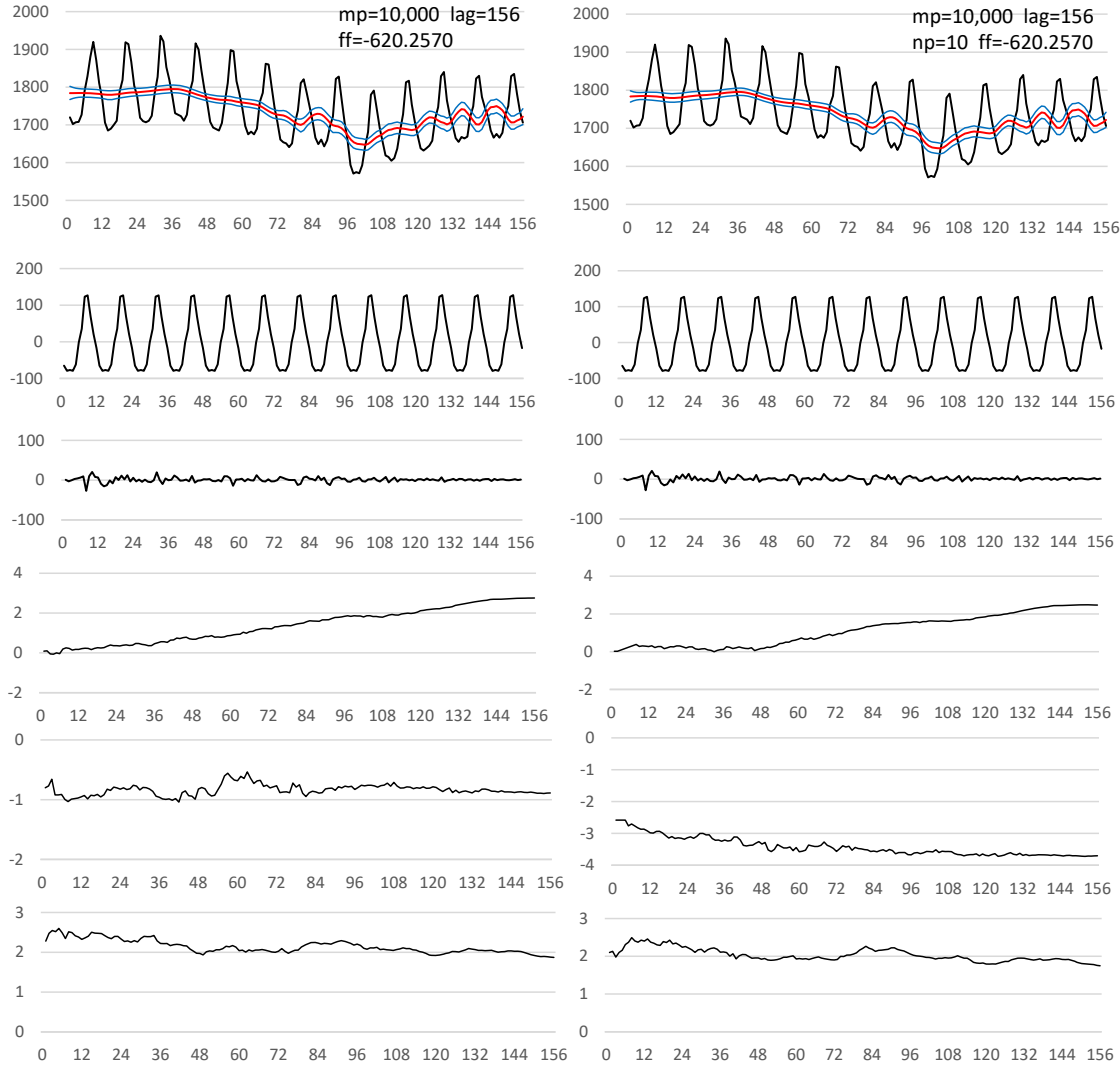


Figure 11: Seasonal adjustment by RB-SOF modeling, Left: particle filter with $mp=10,000$, right: non-Gaussian filter with $k_1 = k_2 = k_3 = 31$.

that the variance of the trend increases with time, the variance of the existing components is almost constant, and the variance of the observed noise decreases slightly with time.

Table 5 compares the sum of squares of the estimation errors of the trend and seasonal components and cpu-time for the seasonal adjustment case. From top to bottom, the results are shown for the regular particle filter (PF-SOF), the Rao-Blackwellized particle filter (RB-PF-SOF), and the Rao-Blackwellized particle filter approximated by the 2-step method. The 2-step approximation method is discussed later.

Comparing PF and RB-PF, it can be seen that the same level of calculation accuracy can be achieved with about 1/100th the number of particles by Rao-Blackwellization. Unfortunately, however, the cpu-time shows that even though the number of particles decreases, the computation time remains almost the same, and in some cases it even increases. This phenomenon is clearly shown in Figure 12, where the green line indicates the simple particle filter and the red line indicates Rao-Blackwellized particle filter. The left figure shows the relationship between the number of particles and estimation accuracy, indicating that only 1/100 or less particles are needed to obtain the same accuracy. However, looking at the relationship between cpu-time and

Table 5: Comparison of sum of squared errors of trend and seasonal components and cpu-time for seasonal adjustment. PF-SOF: Ordinary particle filter, RB-SOF: Rao-Blackwellized particle filter, 2-step RB-SOF: approximated 2-step method for RB-SOF.

Filter Method	mp	squared estimation errors			cpu-time	
		log-lik	Filter	Smoother	Filter	Smoother
PF-SOF	1,000	-626.803	4.1993	4.8192	0.078	0.250
	10,000	-616.856	0.7288	1.3815	0.797	2.313
	100,000	-614.222	0.2524	0.6708	7.938	22.469
	1,000,000	-613.199	0.0702	0.2941	79.234	223.906
RB-PF-SOF	10	-676.464	13.4550	9.1591	0.281	0.313
	100	-634.399	3.5471	2.1087	2.656	2.969
	1,000	-623.006	0.7494	0.4368	29.219	32.359
	10,000	-620.331	0.1224	0.0829	296.578	327.719
2-step RB-SOF np=11	10	-677.402	15.8960	11.0219	0.016	0.063
	100	-634.399	3.6567	2.1387	0.156	0.063
	1,000	-622.300	0.6501	0.3899	1.625	0.047
	10,000	-620.407	0.1258	0.0880	16.266	0.047
	100,000	-620.015	0.0310	0.0413	161.719	0.047

estimated accuracy on the right side, the red and green lines cross each other, and there is no significant superiority or inferiority.

The reason for this is that in RB, the Kalman filter must be computed with different parameters for each particle, and when the dimension of the state vector is high, the computational complexity of this part becomes dominant.

Considering that the accuracy of estimating structural parameters such as variance is not as necessary compared to estimating the state, it is possible that the calculations are repeated more rigorously than necessary. Therefore, in the following, we examine how to calculate the approximate posterior distribution by the 2-step method.

4.4 2-step Method for Approximating the Rao-Blackwellized Particle Smoother

The following two points are considered to be the causes of the increase in computation time when Rao-Blackwellization is performed strictly when the dimension of the state space model that can be computed by the Kalman filter is high.

1. The need to repeat Kalman smoothing for each particle in the particle filter.
2. When smoothing by the particle filter is realized by a particle-preserving method, it is necessary to resample all particles from the start of the time series at each time in preparation for the smoothing.

Possible ways to alleviate the second problem above include not performing resampling at all times, but only when necessary for a certain criterion, or smoothing with a two-filter method instead of fixed lag smoothing, but we will not consider these methods here because they complicate the problem.

[2-step Method]

In the following, np is the number of percentile points to express the posterior distribution. Given np , the np percentile points corresponding to the probabilities are determined as $p_i = (i + 0.5)/np$. For example, if $np = 5$, p_i is given by 0.1, 0.3, 0.5, 0.7, 0.9.

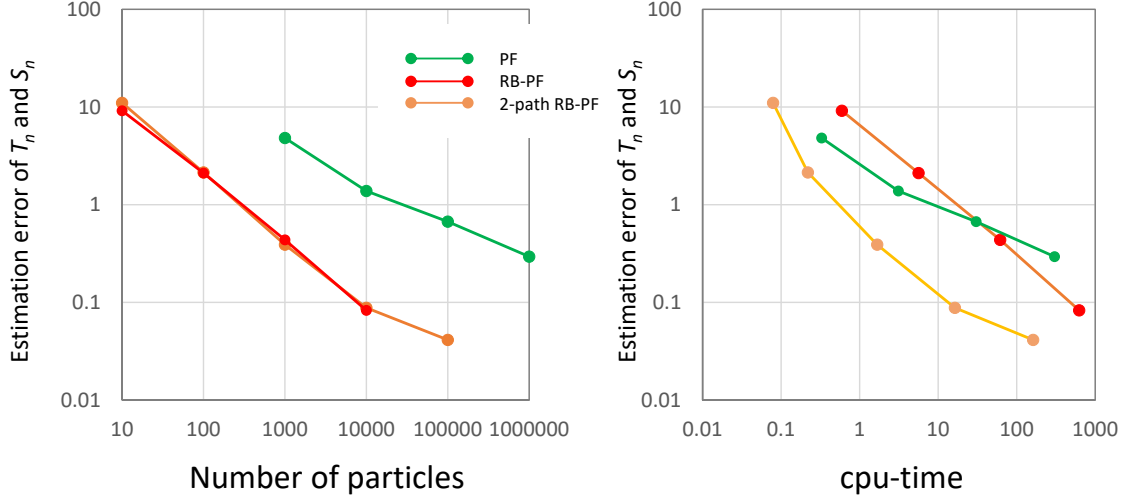


Figure 12: Number of particles or cpu-time vs. estimation errors of the trend and seasonal components.

1. Perform the RB particle filtering. At this time, fixed lag smoothing is performed for only the parameter vector θ_n by setting $\text{LAG}=\text{N}$, the data length, but past history of the state $x_{n|j}$, $j = 1, \dots, n$ and the variance covariance matrix $V_{n|j}$, $j = 1, \dots, n$ obtained by the Kalman filter are not preserved.
2. From the obtained posterior distribution of the parameter $\theta_{n|N}$, the percentage points at each time $n = 1, \dots, N$, the values of the parameters θ_n^j corresponding to the np percent points, p_i , $i = 1, \dots, np$, are computed for each time $n = 1, \dots, N$.
3. For $i = 1, \dots, np$, using the pairs of parameters $(\tau_{1n}^2(i), \tau_{2n}^2(i), \sigma_n^2(i))$, Kalman filter and smoothing are performed to obtain the mean value functions, T_n^i and S_n^i , for $n = 1, \dots, N$ and $i = 1, \dots, np$.
4. Obtain the approximated posterior mean function by the simple average of the np trend and seasonal components obtained in the previous step.

The right side of Figure 11 shows the results obtained by the 2-step approximation. Although the estimates of the variance of the seasonal component are different, the trend and seasonal components are similar to the estimates shown on the left side of the figure.

The bottom five rows of Table 5 show the estimation error and cpu-time by 2-step approximation with $np=11$. In many cases, the errors are a little larger because of the approximation, but the filter cpu-time is less than 1/10. It is also noteworthy that the cpu-time of smoothing does not increase at all when mp is increased because np is fixed. As a result, even if the number of particles is increased by a factor of 10 ($mp=100,000$), the cpu-time takes only 1/3 of the time required when $mp=10,000$ for RB-PF.

Since the optimal value of the number of percentage points, np , remains unclear, a Monte Carlo experiment was conducted to investigate this issue. Table 6 presents the sum of squared errors for the trend and seasonal components across different values of np and Lag, under the conditions of $mp=1,000$ and $mp=10,000$.

The case $np=1$ corresponds to the posterior mean estimator. Red-highlighted values in the table indicate those near the minimum error point. The results suggest that satisfactory approximations are achieved around $np=11$, beyond which increasing np yields little additional

Table 6: Effect of np and LAG in two-way smoothing. Left: $mp=1,000$, right: $mp=10,000$

np	Lag					Lag				
	24	48	72	96	156	24	48	72	96	156
1	0.6204	0.4781	0.4643	0.4874	0.4800	0.3322	0.1541	0.1512	0.1637	0.1428
3	0.5484	0.3961	0.3733	0.3828	0.3997	0.1317	0.1317	0.1159	0.1067	0.0921
5	0.5326	0.3884	0.3671	0.3759	0.3972	0.2893	0.1280	0.1098	0.1018	0.0906
11	0.5290	0.3826	0.3600	0.3600	0.3899	0.2852	0.1244	0.1067	0.1003	0.0880
21	0.5261	0.3815	0.3600	0.3699	0.3886	0.2834	0.1237	0.1055	0.0988	0.0871
51	0.5252	0.3809	0.3595	0.3700	0.3601	0.2822	0.1233	0.1053	0.0986	0.0873

improvement. Furthermore, the choice of the Lag value appears to have a greater influence on the results than the choice of np .

For example, when the number of particles is $mp=10,000$, Lag = 156 (the number of data points) is acceptable. However, when $mp=1,000$, Lag = 72 provides better results.

Finally, Figure 12 illustrates the impact of the 2-step approximation (indicated in orange). As shown in the left panel, the relationship between the number of particles and estimation accuracy remains largely unchanged, even when the 2-step approximation is applied. However, as depicted in the right panel, the computation time is significantly reduced, by approximately 1/10 to 1/40.

5 Conclusion

In this paper, we explore a self-organization method that simultaneously performs state and parameter estimation using a state-space model, with trend estimation and seasonal adjustment as illustrative examples. This method offers the advantage of being a form of Bayesian estimation that avoids the repeated likelihood calculations required by maximum likelihood estimation. Moreover, it enables simultaneous state and parameter estimation through a single filtering and smoothing process. However, a significant drawback arises: even if the original state-space model is linear Gaussian-allowing the use of the Kalman filter-the self-organized state-space model becomes nonlinear, rendering the Kalman filter inapplicable.

For trend estimation, the self-organized state-space model has a relatively low dimensionality of two or three. In such cases, a particle filter or a non-Gaussian filter based on numerical integration can be employed to obtain a nearly accurate smoothed distribution without significant computational challenges. In contrast, for seasonal adjustment models, the standard state vector dimension is 13, and the parameter vector dimension is 3, resulting in a self-organizing state-space model with 16 dimensions. In this higher-dimensional setting, non-Gaussian filters are impractical, and while particle filters can be applied, achieving high estimation accuracy requires an extremely large number of particles.

To address this issue, the estimation accuracy can be enhanced using Rao-Blackwellization, which leverages the partial linearity of the model. For trend estimation problems, this approach achieves comparable accuracy with fewer than 1/100 of the particles required by standard methods. Similarly, for seasonal adjustment models, using a particle filter for the parameter vector achieves comparable accuracy with approximately 1/100 of the particles. However, in the case of seasonal adjustment models with a 13-dimensional linear state, while the number of particles is significantly reduced, the computational time is not similarly reduced.

To overcome this limitation, we adopt the 2-step approximation method. In this approach, the posterior distribution of the parameters is first estimated, and the state vector is then

estimated using the Kalman filter and smoothing, conditioned on the posterior distribution. Monte Carlo evaluations demonstrate that this method achieves near-zero estimation error while reducing computational time to only a fraction of a second.

References

- [1] Anderson, B.D.O., and Moore, J.B. (1979). *Optimal Filtering*, New Jersey, Prentice-Hall.
- [2] Doucet, A., Godsill, S. and Andrieu, C. (2000). On sequential Monte Carlo sampling methods for Bayesian filtering, *Statistics and Computing*, **10**, 197–208.
- [3] Doucet, A., de Freitas, N., Murphy, K. and Russell S., (2000). Rao-Blackwellised Particle Filtering for Dynamic Bayesian Networks, *Uncertainty in Artificial Intelligence Proceedings*, 176–183.
- [4] Doucet, A., de Freitas, N., and Gordon, N., (2001). *Sequential Monte Carlo Methods in Practice*. Springer-Verlag, New York.
- [5] Durbin, J., and Koopman, S. J., (2012). *Time Series Analysis by State Space Methods*, Vol.38. Oxford Statistical Science, Croydon, UK.
- [6] Gordon, N. J., Salmond, D. J., and Smith, A. F. M., (1993). Novel approach to nonlinear/non-Gaussian Bayesian state estimation, *IEE Proceedings-F*, **140**, 107–113.
- [7] Grisetti, G., Stachniss, C., and Burgard, W. (2007). Improved techniques for grid mapping with rao-blackwellized particle filters. *IEEE transactions on Robotics*, **23**(1), 34–46.
- [8] Grisetti, G., Tipaldi, G. D., Stachniss, C., Burgard, W., and Nardi, D. (2007). Fast and accurate SLAM with Rao-Blackwellized particle filters. *Robotics and Autonomous Systems*, **55**(1), 30–38.
- [9] Harrison, P.J. and Stevens, C.F. (1976), Bayesian Forecasting (with discussion), *Journal of the Royal Statistical Society*, Series B, Vol. 34, 1-41.
- [10] Hendeby, G., Karlsson, R. and Gustafsson, F., (2010). The Rao-Blackwellized Particle filter: A Filter Bank Implementation. *EURASIP Journal on Advances in Signal Processing*, **2010**, Article ID 724087, 1–10.
- [11] Khan, Z., Balch, T., and Dellaert, F. (2004). A rao-blackwellized particle filter for eigen-tracking. *Proceedings of the 2004 IEEE Computer Society Conference on Computer Vision and Pattern Recognition*, **2**, II–II).
- [12] Kitagawa, G. (1987), Non-Gaussian State Space Modeling of Nonstationary Time Series, *Journal of American Statistical Association*, Vol.76, No.400, 1032-1064.
- [13] Kitagawa, G. (1988), Numerical Approach to Non-Gaussian Smoothing and its Applications, *Computing Science and Statistics; Proceedings of the 20th Symposium on the Interface*, eds. E.J. Wegman, D.T. Gantz and J.J. Miller, 379-388.
- [14] Kitagawa, G., (1993). A Monte Carlo filtering and smoothing method for non-Gaussian nonlinear state space models, *Proceedings of the 2nd U.S.-Japan Joint Seminar on Statistical Time Series Analysis*, 110–131.

- [15] Kitagawa, G., (1996). Monte Carlo filter and smoother for non-Gaussian nonlinear state space model, *Journal of Computational and Graphical Statistics*, **5**, 1–25.
- [16] Kitagawa, G., (2010). *Introduction to Time Series Modeling*, Chapman & Hall/CRC Press, New York.
- [17] Kitagawa, G., (2014). Computational aspects of sequential Monte Carlo filter and smoother. *Annals of the Institute of Statistical Mathematics*, **66**, 443–471.
- [18] Kitagawa, G. and Gersch, W.(1984). A Smoothness Priors-State Space Approach to the Modeling of Time Series with Trend and Seasonality, *Journal of the American Statistical Association*, 79, No.386, 378-389.
- [19] Kitagawa, G., and Gersch, W., (1996). *Smoothness Priors Analysis of Time Series*, Springer-Verlag, New York.
- [20] Prado, R. and West, M. (2010). *Time Series Modeling, Computation, and Inference*, Chapman & Hall, CRC Press, Florida.
- [21] Särkkä, S., Vehtari, A. and Lampinen, J., (2007). Rao-Blackwellized Particle filter for multiple target tracking, *Information Fusion*, **8**(1) 2–15.
- [22] Shumway, R.H., and Stoffer, D.S., (2000). *Time Series Analysis and Its Applications*, Springer Texts in Statistics, Springer, New York.
- [23] West, M. and Harrison, J. (1989). *Bayesian Forecasting and Dynamic Models* , Springer Series in statistics, Springer-Verlag, New York.